Intracellular movement of protein aggregates reveals heterogeneous inactivation and resuscitation dynamics in stressed populations of *Escherichia coli*

Sander K. Govers[a], Elisa Gayan[a] and Abram Aertsen[a#]

[a]Laboratory of Food Microbiology, Department of Microbial and Molecular Systems (M²S), Faculty of Bioscience Engineering, KU Leuven, Leuven, Belgium

Running title: Heterogeneity in stressed bacterial populations

[#]Corresponding author: Abram Aertsen

Kasteelpark Arenberg 23, bus 2457, 3001 Leuven, Belgium,

tel. +32 16 32 17 52

fax +32 16 32 19 60

Abram.Aertsen@biw.kuleuven.be

Originality-Significance statement

The authors confirm that all of the reported work is original. By taking into account the intracellular movement of protein aggregates as a proxy of the metabolic status of individual cells, this study provides an unsurpassed resolution of the heterogeneous inactivation and resuscitation dynamics in stressed clonal populations of *Escherichia coli*.

Summary

Inactivation of bacterial pathogens is of critical importance in fields ranging from antimicrobial therapy to food preservation. The efficacy of an antimicrobial treatment is often experimentally determined through viable plate counts that inherently provide a poor focus on the mechanisms and distribution of (sub)lethal injury and subsequent inactivation or resuscitation behavior of the stressed cells, which are increasingly important features for the proper understanding and design of inactivation strategies. In this report, we employ a live cell biology approach focusing on the energy-dependent motion of intracellular protein aggregates to investigate the heterogeneity within heat stressed *Escherichia coli* populations. As such, we were able to identify differential dynamics of cellular resuscitation and inactivation that are impossible to distinguish using more traditional approaches. Moreover, our data indicate the existence of late-resuscitating cells that remain physiologically active and are able to persist in the presence of antibiotics before resuscitation.

Introduction

While distinct cellular differentiation events have been uncovered that can impose a biologically meaningful phenotypic heterogeneity upon clonal microbial populations (e.g. formation of persisters, decision to sporulate in *Bacillus subtilis*, bistability in the central carbon metabolism of *E. coli*; (Balaban et al., 2004; Veening et al., 2008; Ryall et al., 2012; Kotte et al., 2014; Ackermann, 2015)), little is known about the phenotypic heterogeneity displayed within isogenic populations as a result of severe stress. Nevertheless, it might be anticipated that cells within clonal populations exposed to hostile environments or inimical treatments incur differing degrees of injury and therefore display potentially variable behavior (Niven et al., 2008; Wesche et al., 2009; Govers and Aertsen, 2015). In fact, such phenotypic heterogeneity in stressed microbial populations would be of importance in almost every context of microbial inactivation, ranging from environmental insults to the preservation of foods (Fellows, 2000; Pasha et al., 2014) and the treatment of microbial infections (Gefen and Balaban, 2009). Moreover, a comprehensive understanding of the distribution and management of (sub)lethal injury throughout a stressed population could be crucial for the design of novel microbial inactivation strategies.

However, the heterogeneity in cellular injury incurred throughout a clonal population and the corresponding individual inactivation or resuscitation dynamics of stressed cells so far remain elusive due to the fact that insights into microbial inactivation and survival tend to stem from viable plate count methods that yield a misleadingly straightforward binary live/dead response based upon the premise that each individual surviving cell, when placed on nutrient media, should be able to grow, divide and give rise to a macroscopically visible colony (Booth, 2002; Davey, 2011). Moreover, even single-cell level approaches based on the combination of fluorescent dyes and flow cytometry to assess the distribution of microbial viability and other cellular attributes throughout the population (Joux and Lebaron, 2000;

Strauber and Muller, 2010) lack the proper temporal resolution to determine whether or not certain discernable cellular subgroups eventually commit to growth and division. In contrast, time-lapse fluorescence microscopy (TLFM) allows probing the individual behavior and physiology of a large number of cells simultaneously through time, thereby enabling the acquisition of information about an individual cell's actual (sub)lethal injuries and corresponding behavior throughout inactivation or resuscitation, as well as the heterogeneity with which these events occur throughout the stressed population (Booth, 2002; Ingham et al., 2008; Niven et al., 2008; Koutsoumanis and Lianou, 2013; Govers and Aertsen, 2015).

Employing TLFM, we have previously shown that *Escherichia coli* populations subjected to high hydrostatic pressure stress not only displayed increased cellular inactivation, but also longer and more heterogeneous resuscitation times with increasing pressure intensities (Govers and Aertsen, 2015). Moreover, we showed that increased pressure led to increased dispersal of intracellular protein aggregates (PAs, unfolded and misfolded proteins which aggregate into larger insoluble structures through hydrophobic interactions (Dobson, 2003); made fluorescently tractable through an IbpA-YFP fusion; (Lindner et al., 2008)), of which the reassembly process in individual cells appeared to be linked to their resuscitation times (Govers et al., 2014; Govers and Aertsen, 2015). In this report, we expand these live cell biology approaches by examining single cells of *E. coli* MG1655 *ibpA-yfp* populations subjected to heat treatments of different intensities, while at the same time monitoring the movement of their intracellular PAs. Integrating information on PA movement, which we first show to be dependent on metabolic activity due to the glass-like properties of the bacterial cytoplasm (Parry et al., 2014), with growth capacity at the single-cell level allowed an unprecedented in-depth analysis and characterization of individual cellular resuscitation dynamics in severely stressed clonal populations.

Results

Intracellular PA movement serves as a proxy for the metabolic status of the cell

Although intracellular PA (re)assembly and movement was initially thought to be strictly diffusion-based and thus energy-independent (Winkler et al., 2010; Coquel et al., 2013), more-detailed insights into the physical nature of the bacterial cytoplasm and its glass-like properties have indicated that the mobility of such larger intracellular structures is progressively constrained with increasing size, and that cellular metabolism is required to fluidize the cytoplasm, in order to allow these structures to escape their local environment and explore larger regions of the cytoplasm (Parry et al., 2014). Recently, polar segregation of PAs has been shown to be hampered in conditions of increased cytoplasmic viscosity (Oliveira et al., 2015), indicating the latter, modulated by factors such as metabolic activity, temperature and osmolality (Weber et al., 2012; Parry et al., 2014; Oliveira et al., 2015), can indeed affect PA behavior. In order to fully examine the impact of these metabolism-dependent glass-like dynamics of the bacterial cytoplasm on PAs, we monitored live *E. coli* MG1655 *ibpA-yfp* cells, in which PAs are fluorescently traceable (Lindner et al., 2008), in different environments and quantified their macromolecular motion (Fig. 1).

In control conditions (i.e. untreated stationary phase cells monitored in a nutrient-rich environment before growth resumption), PAs displayed marked movement and were able to sample the entire cytoplasm within minutes (Fig. 1A and D). However, upon addition of CCCP (carbonyl cyanide m-chlorophenyl hydrazine), an oxidative phosphorylation uncoupling agent that was previously shown to reduce cellular energy without affecting viability (Winkler et al., 2010; Govers et al., 2014), PA mobility drastically decreased and PAs became spatially confined to a given intracellular region (Fig. 1B and E). Moreover, when cells were exposed to this uncoupler in a nutrient-free environment, attenuating other

cellular sources of energy such as substrate-level phosphorylation in glycolysis, movement appeared to cease completely (Fig. 1C and F). These initial observations were confirmed by calculating the one-dimensional (along the long cell axis) ensemble-averaged mean squared displacements (MSDs) over a large number of trajectories for each of these conditions (n = 267-480) (Fig. 1G), indicating that PA mobility is indeed proportionally compromised in metabolically reduced or inactive cells. Furthermore, even in exponentially growing cells, where PA mobility is more limited due to the smaller nucleoid-free regions (the cell poles) (Winkler et al., 2010; Coquel et al., 2013; Govers et al., 2014), a similar albeit smaller effect could be observed (Fig. S1). Taken together, these results demonstrate PA movement to require metabolic activity and as such can be considered as indicative (and thus a proxy) for the metabolic status of the cell.

Intracellular PA movement reveals heterogeneity in stressed populations

In a subsequent stage, we exploited this metabolism-dependent PA movement to characterize bacterial inactivation and resuscitation after heat treatment at an unprecedented resolution. We exposed *E. coli* MG1655 *ibpA-yfp* populations to varying heat intensities (for 15 min) and subsequently monitored them using time-lapse fluorescence microscopy. In line with previous inactivation experiments (Standaert et al., 2007; Black et al., 2010; Govers and Aertsen, 2015), increasing temperature led to increased bacterial inactivation (Fig. 2A). Whereas almost all control cells were able to resuscitate (91.6 % ± 6.6 of observed cells), defined here as the ability of a cell to resume growth and subsequently divide within 8 hours after heat treatment, this fraction became significantly smaller with increasing heat intensities (61.5 % ± 6.0 after 51 °C, 57.9 % ± 4.2 after 52 °C and 50.1 % ± 3.9 after 53 °C, respectively), with only a very limited number (0.8 % ± 0.5 after 54 °C) or no (after 55 °C, with the detection limit of these samples ranging from 0.3 to 0.5 %) cells resuscitating after exposure to high heat intensities (Fig. 2A). In addition, increased heat intensity resulted in longer and more heterogeneous (Pearson's r = 0.9922, p-value = 8.94×10^{-5})

resuscitation times (defined here as the time a cell needs to gain a microscopically detectable increase in cell length) of resuscitating cells (Fig. 2A-B). The average resuscitation time for single cells in untreated control samples was 21.3 min ± 0.9, and this average increased to 48.8 min ± 9.8, 52.5 min ± 10.4, 104.8 min ± 25.7 and 319.3 min ± 63.1 min for resuscitating cells exposed to 51, 52, 53 and 54 °C, respectively (Fig. 2A-C).

When additionally taking into account intracellular PA movement, we surprisingly observed that none of the heat exposed cells displayed immediate PA movement, which might suggest that even the resuscitating cells initially lack the metabolic activity required to allow PA movement. This is in contrast to the unstressed control population, in which all PA-moving cells already display PA movement from the start of TLFM recordings (data not shown). Subsequently, at different times after heat treatment, a fraction of cells resumed PA movement, although not all of them were also able to resuscitate (i.e. resume growth and subsequently commit to division) (Fig. 2C, Fig. 3). While this latter fraction of cells was negligible in control populations (ca. 0.8 %), it increased significantly after exposure to stress (5.2-9.0 %), especially when taking into account the declining number of resuscitating cells with increasing temperature (Fig. 3). As such, monitoring PA movement clearly allows an improved differentiation within resuscitating and succumbing cells.

Intracellular PA movement increases the resolution of individual cellular fates in stressed populations

In order to examine this apparent heterogeneity within stressed populations in more detail, we quantitatively scrutinized the dynamics in individual cells of populations exposed to a heat treatment of 53 °C (15 min) in terms of cellular integrity, PA movement/metabolic activity, and resuscitation capacity (Fig. 4A).

The subpopulation of cells (50.1 %) able to resuscitate always initiated (and sustained) PA movement before resuming growth, with on average a 48.5 ± 25.4 min difference between both events (Fig. 4C-F). Although within this subpopulation a significant correlation was observed between the time needed to initiate PA movement and the time needed to resume growth (Fig. 4C-E, Pearson's r = 0.3479, p-value = 1.94×10^{-5}), this correlation was not particularly strong, indicating that other repair processes are likely also of importance during bacterial resuscitation.

Another subpopulation (6.8 %), however, was apparently unable to resuscitate despite the fact that they managed to initiate PA movement at some point (Fig. 4G-I and L), suggesting that the resumption of PA movement itself is not a good proxy for the eventual cell fate. Moreover, the timing at which initiation of PA movement occurs is not a good proxy for cell fate either, since the distribution of this parameter was not significantly different between resuscitating and non-resuscitating (PA moving) cells (Kolmogorov-Smirnov test, $\alpha = 0.05$) (Fig. 4B-C). While a small fraction (1.2 % of the total number of observed cells) of this subpopulation remained metabolically active during the entire course of TLFM recording (i.e. until at least 8 hours after heat treatment; Fig. 4L), most cells (5.6 % of the total number of observed cells) ceased PA movement well before (Fig. 4A and G-I), indicating they embarked on resuscitation but eventually lost the necessary metabolic activity required to fluidize their cytoplasm and succumbed. The latter was often accompanied by some form of structural decay (Fig. 4G-H).

Finally, a large subpopulation of cells (43.1 %) was unable to resuscitate and showed no initiation of PA movement (Fig. 4J-K). Frequently, these cells also suffered structural decay, similar to the cells that initiated but subsequently ceased PA movement (Fig. 4J). It is noteworthy that the severity and dynamics of structural decay were heterogeneous as well, ranging from partial to complete cellular lysis occurring

either concomitantly with or at different times after heat treatment or loss of PA movement (Fig. 4G-H and J), further underscoring the heterogeneous impact of stress on bacterial populations.

Interestingly, re-analysis of a previous dataset (Govers and Aertsen, 2015), in which *E. coli* MG1655 *ibpA-yfp* cells were exposed to HHP (300 MPa, 15 min, 20 °C), revealed a similar heterogeneity in inactivation and resuscitation dynamics (Fig. S2). Similar to cells after heat treatment, these cells, in which the PAs were dispersed by the exposure to HHP and subsequently reassembled (Govers and Aertsen, 2015), could be divided into subgroups of resuscitating or non-resuscitating, and displaying PA movement or not (Fig. S2).

Metabolically active but non-resuscitating cells can perform gene expression and protein translation

In order to further interrogate the operational capacities of those metabolically active (i.e. PA moving) but non-resuscitating cells in terms of transcription and translation, we equipped the *E. coli* MG1655 *ibpA-yfp* strain with a vector (pTrc99A-P_{trc}-*mCer3*) allowing the inducible expression (upon addition of IPTG) of a cyan fluorescent protein (mCerulean3). After heat treatment (53 °C, 15 min), these cells, grown overnight without inducer, were placed under the microscope on ampicillin- (for maintenance of the expression vector) and IPTG-containing (1 mM) agarose pads and their subsequent resuscitation was monitored. In these conditions, a similar heterogeneous pattern of resuscitating and non-resuscitating, PA moving and non-moving cells could be observed. As expected, all resuscitating cells can clearly commit to transcription and translation, indicated by the increase in total cellular cyan fluorescence (Fig. 5A). In contrast, while some of the non-resuscitating but metabolically active cells clearly initiated gene expression (Fig. 5B-C), others were not able to initiate any detectable levels of gene expression. These

findings therefore suggest that in stressed cells metabolic activity (as judged by intracellular PA movement) does not necessarily warrant resumption of transcriptional and/or translational capacity.

Metabolically active but non-resuscitating cells are able to persist in the presence of ampicillin

Since cells that remained metabolically active but were not able to commit to growth and division (within the 8 h time frame of our TLFM recordings) represent a peculiar fraction of which some cells might even resume transcription and translation, we set forward to examine the eventual fate of this subgroup more closely. More specifically, we exposed stressed (53 °C, 15 min) MG1655 *ibpA-yfp* cells to ampicillin (100 µg/ml) during their resuscitation, thereby selectively eliminating all cells resuming growth (Joers et al., 2010; Fridman et al., 2014) and preventing these non-resuscitating cells from being overgrown by other resuscitating cells within the same microscopy field (Fig. 6A-B). As anticipated, unstressed control cells almost immediately lysed upon exposure to the antibiotic (Fig. 6A), whereas none of the stressed/resuscitating cells lysed immediately, but only after PA movement had resumed and cells attempted to resume growth (Fig. 6B). A period was thus observed during which stressed cells, in contrast to their unstressed counterparts, could survive and thus persist in the presence of ampicillin up to the point of growth recovery.

As such, we were able to specifically monitor those cells initially identified as metabolically active but unable to resume growth and subsequent division (and thus insensitive towards the ampicillin) for longer periods of time after heat treatment (53°C, 15 min). More specifically, this was accomplished by extending an initial observation period of 8 h directly after heat treatment (allowing the selective identification of cells displaying this behavior) with two extra observation periods at 24 and 48 h after treatment (allowing the assessment of their eventual fate). The latter two observation periods hereby served to establish

whether or not these cells had maintained their metabolic activity and/or structural integrity. Employing this setup, in which we found a similar fraction of cells (1.9 % of visible cells, n = 1491) able to sustain PA movement (without resuming growth and subsequent division) after 8 h of observation as in previous experiments without the addition of ampicillin (1.2 % of visible cells, n = 462; Fig. 4A), allowed us to observe all these cells to a point in time where they no longer displayed PA movement (Fig. 6C-G). Interestingly, extended monitoring of these metabolically active but seemingly non-resuscitating cells revealed that ca. 20 % of them retained PA movement for at least 24 h after heat stress, while after 48 h no such cells could be detected anymore (Fig. 6G). Whereas some cells had ceased PA movement without losing their structural integrity (25 % of remaining PA-moving cells; Fig. 6C-D), suggesting they no longer exhibited the necessary metabolic activity to sustain PA movement and succumbed, others had completely lost their structural integrity (75 % of remaining PA-moving cells; Fig. 6E-F). Since it is hard to unambiguously attribute loss of cellular integrity to either cell death-mediated structural decay on the one hand or growth-mediated lysis by ampicillin on the other, the actual fate of such cells still remained obscure.

In order to further address this issue, we exposed both unstressed control cells and heat (53°C, 15 min) stressed cells to ampicillin after (1/1000) dilution into fresh LB medium, and withdrew samples for viable count measurement through colony formation at varying points in time (Fig. 6H). Whereas most control cells rapidly lost viability, with only the typical persister fraction remaining after 4 hours (Gefen et al., 2008; Joers et al., 2010; Orman and Brynildsen, 2015), stressed cells, in agreement with their resuscitation pattern observed with TLFM, displayed a much more heterogeneous persistence pattern (Fig. 6H). Indeed, resuscitating cells within this stressed population were initially completely insensitive to the antibiotic, after which they gradually became sensitized towards the ampicillin at a much slower pace than observed for unstressed control cells (Fig. 6H). Especially in the time window from 2 to 8 hours after heat treatment,

a significantly larger persister fraction could be found in stressed populations compared to their unstressed counterparts. Moreover, after 8 hours in the presence of ampicillin, ca. 0.2 % of stressed cells still retained the ability to grow and resuscitate, suggesting that a significant fraction of the previously observed metabolically active but non-resuscitating cells is indeed able to give rise to a macroscopically visible colony.

Taken together, these findings suggest that the persistence capacity of stressed cells is to a large extent determined by their resuscitation time and that a fraction of the cells identified as metabolically active but non-resuscitating earlier on in the manuscript is still able to resuscitate eventually. In fact, these late resuscitators likely give rise to the late-appearing colonies that are typically observed in plate count assays upon prolonged incubation (also visible in our experimental setup; Fig. 6I).

Discussion

Monitoring the metabolism-dependent motion of intracellular PAs (as visualized by the IbpA-YFP fusion protein (Lindner et al., 2008)) increased the resolution of our insights into the events and cell-to-cell heterogeneity incurred within stressed clonal populations of *E. coli*, and allowed us to discriminate among (i) cells resuming metabolic activity and resuscitating, (ii) cells resuming metabolic activity but not (readily) resuscitating, (iii) cells transiently resuming metabolic activity but succumbing, and (iv) succumbed cells not resuming metabolic activity. The existence of and variation within these different possible cellular outcomes clearly underscores that, for reasons that are often still obscure, cellular injury by heat (or hydrostatic pressure) is very unevenly distributed or perceived among sibling cells.

Upon scrutinizing the resuscitating population, we surprisingly observed that none of the cells displayed PA movement directly after stress. This observation was in stark contrast to the behavior of unstressed cells which readily (and uniformly) resumed PA movement upon placement on agarose pads containing fresh LB medium. Although the exact underlying cause for this observation currently remains elusive, it might reflect heat stress mediated perturbation of cellular energy metabolism (Soini et al., 2005; Jozefczuk et al., 2010; Ye et al., 2012) that needs to be overcome in order for PA movement to initiate and resuscitation to occur. While the time needed for resumption of metabolic activity was highly variable within the resuscitating fraction, it did not strongly correlate with the variability in individual resuscitation times, suggesting processes other than resumption of metabolic activity to also play a key role in cellular recovery.

The non-resuscitating population could be divided into more qualitatively distinct subpopulations, with the majority of cells never resuming metabolic activity, suggesting their immediate inactivation. This is in contrast to the fraction of non-resuscitating cells that do manage to resume metabolic activity, and thus seem to initiate or mount a resuscitation process, but subsequently fail to sustain it and succumb to the injury. As such, monitoring intracellular PA movement clearly allows to uncover the often cryptic heterogeneity and dynamics present in the non-resuscitating fraction, with cells being immediately inactivated or rather succumbing at an individual pace after exposure to stress.

An interesting subpopulation comprises those cells that seem to commit to sustained PA movement (suggesting resuscitation to be in progress) but refrain from division throughout the 8 h of post-stress TLFM monitoring, despite the fact that some of them seem to display the ability to engage in protein synthesis. While it is hard to unambiguously pinpoint the eventual fate of these cells after longer periods of time, our observations suggest that at least a fraction of them eventually resuscitates completely. As a

consequence, such cells are prone to escape detection by traditional plating while their metabolic activity and resuscitation potential might still compromise treatment efficacy.

Although this phenomenon requires further scrutiny, these delayed resuscitators seem to establish a gap with the first wave of resuscitators that (despite their variability) already commit to growth and subsequent division well before the first 8 h post-stress. Intuitively, however, there seems to be no reason why the level of cellular injury and the corresponding resuscitation time should display such a discontinuous distribution. As such, it is tempting to speculate that some survivors might postpone resuscitation longer than is required in terms of their incurred injury. In fact, the observed cell-to-cell variability in resuscitation could be more than an unfortunate artefact of the inimical treatment, and reveal a bet-hedging strategy that allows cellular survival in future hostile environments, reminiscent of the superdormancy-mediated heterogeneity observed in the germination of endospore populations of *Bacillus* and *Clostridium* species (Stringer et al., 2005; Ghosh and Setlow, 2009; Ghosh et al., 2012). Importantly, resuscitating cells were able to persist in the presence of ampicillin, and only became sensitized towards the antibiotic when attempting to resume growth. In this respect, sublethal injury is found to induce a similar cellular behavior as that displayed by viable but nonculturable (VBNC) and persister cells (Ayrapetyan et al., 2015), perhaps underscoring a more fundamental resemblance among these states. This observation not only demonstrates the well-known interplay between environmental stress and persistence (Ayrapetyan et al., 2015), but also supports recent findings indicating the lag phase is an important factor (as well as an evolvable attribute) to consider when examining microbial persistence phenomena (Fridman et al., 2014).

While PA movement provides an easily discernable microscopic proxy for cellular metabolic activity, its use is nevertheless subjected to some caveats. As such, it is clear from our results that a single

instantaneous measurement of PA movement (or lack thereof) is not sufficient to properly predict cellular fate in stressed populations, since even resuscitating cells show an initial period of lack of PA movement, while dying cells might still transiently display PA movement. Furthermore, the time needed for resumption of metabolic activity is a poor proxy of eventual resuscitation as well, since dying (i.e. with transient PA movement) and resuscitating cells display roughly the same variability in this respect. In addition, accurate measurements of PA movement likely depend on aggregate size, given the propensity of the bacterial cytoplasm to, depending on its metabolic status, disproportionally constrain cytoplasmic components with increasing size (Parry et al., 2014). In this light, the use of structures that are smaller and more defined than IbpA-YFP foci, that seem to artificially accumulate IbpA-YFP (Landgraf et al., 2012), could even lead to a more controlled and reproducible measure of dynamic cytoplasmic viscosity in the future. Finally, while intracellular PA movement seems nicely correlated with metabolic activity, it can not be excluded that lack or loss of PA movement might sometimes find its origin in cellular events unrelated to metabolism.

As microorganisms typically tend to face inimical conditions or treatments in both natural and man-made environments, a proper understanding of the physiological heterogeneity and dynamics emerging within stressed microbial populations is of elementary importance. Being able to microscopically differentiate between the various subfractions and their corresponding fate within such populations therefore provides an important basis for future work aiming to study the molecular events and processes occurring in succumbing or resuscitating cells. In turn, this will yield the strategic knowledge required to better anticipate and/or control the dynamics of microbial death and survival in ecological, medical and industrial settings.

Experimental procedures

Strain construction and growth conditions

We employed the *E. coli* MG1655 *ibpA-yfp* strain created in (Govers and Aertsen, 2015), in which expression of the inclusion body binding protein A (IbpA; (Allen et al., 1992)) fused to the yellow fluorescent protein (YFP) makes PAs fluorescently tractable (Lindner et al., 2008). For experiments investigating translational capacity of cells, this strain was equipped with a pTrc99A-P_{trc}-*mCer3* vector, in which a *mCerulean3* amplicon (generated using primers 5'-AGAATTCGTGAGCAAGGGCGAGGAG-3' (Fw) and 5'-AGGATCCTTACTTGTACAGCTCGTCCA-3' (Rev)) was ligated into a pTrc99A backbone using EcoRI (Fw) and BamHI (Rev) restriction sites, allowing the IPTG-inducible production of the cyan fluorescent protein. This plasmid was introduced into *E. coli* MG1655 *ibpA-yfp* by electroporation and selection for ampicillin resistance.

Lysogeny Broth (LB) medium (Miller, 1992; Bertani, 2004) was used either as a broth, or as solid medium after the addition of 2 % agarose (for agarose pads intended for microscopy). Stationary phase cultures were obtained by growing *E. coli* for 15-18 hours in LB broth at 37°C under well aerated conditions (200 rpm on an orbital shaker). For energy depletion experiments, cells were also monitored on phosphate buffered saline (PBS) agarose pads, lacking nutrients. When appropriate, the following chemicals (Applichem, Darmstadt, Germany and Sigma-Aldrich) were added to the medium at the indicated final concentrations: CCCP (carbonyl cyanide m-chlorophenyl hydrazine) (20 μM), ampicillin (100 μg/ml) and IPTG (isopropyl β-D-1-thiogalactopyranoside) (1 mM).

Heat treatment

Cells from stationary phase cultures were harvested by centrifugation (4000 x *g*, 5 min), and resuspended in an equal volume of PBS. Subsequently, a 50 µl portion of resuspended cells was transferred aseptically to a sterile PCR tube and heat treated (at 51, 52, 53 or 54°C) for 15 min in a thermocycler (Westburg, Leusden, The Netherlands). Control samples were also transferred to PCR tubes, but were kept at room temperature for 15 min. After heat treatments, samples were aseptically retrieved from the PCR tubes and subjected to time-lapse fluorescence microscopy as described below.

Time-lapse fluorescence microscopy

For time-lapse fluorescence microscopy, cell suspensions were diluted appropriately, transferred to agarose pads placed on a microscopy slide, and mounted with a cover glass. A Gene Frame (Thermo Scientific) was used to hold the cover glass on the microscopy slide. Time-lapse fluorescence microscopy was performed with a temperature controlled (37 °C; Okolab, Ottaviano, Italy) Ti-Eclipse inverted microscope (Nikon, Champigny-sur-Marne, France) equipped with a 60x objective, a TI-CT-E motorized condenser, a YFP filter (Ex 500/24, DM 520, Em 542/27), a CFP filter (Ex 438/24, DM 458, Em 483/32), and a CoolSnap HQ2 FireWire CCD-camera. Images were acquired every 2 seconds for mean square displacement (MSD) determination, and every 6 min for resuscitation experiments using NIS-Elements software (Nikon). The resulting images were further handled with open source software ImageJ. For further analysis, cell meshes were obtained from the original images using the open source, MATLAB-based software MicrobeTracker (Sliusarenko et al., 2011), and fluorescent spots were detected using the SpotFinder tool within the MicrobeTracker environment.

Particle detection and tracking

Within *E. coli* MG1655 *ibpA-yfp* cells, protein aggregates (PAs) are labelled by the IbpA-Yfp fusion protein and can be detected as fluorescent foci with fluorescence microscopy (Lindner et al., 2008). These fluorescent PA-foci were detected using the SpotFinder tool (Sliusarenko et al., 2011) and their movement was tracked in 2 dimensions for 3 min (x- and y-position in the frame, but also relative to the long (l) and short (d) axes of the cell). However, as in (Parry et al., 2014), only changes in the dimension of the long axis (l) were used for quantitative measurements. Intracellular movement of PAs was quantified by tracking the movement of a large number of foci in live *E. coli* cells and calculating the ensemble-averaged mean square displacement (MSD):

$$MSD = \frac{1}{n}\sum_{i=1}^{n}(l_i(t) - l_i(0))^2$$

where l(t) is the position of a given particle i at time t (relative to the cell's long axis), l(0) is the position of this particle at the beginning of recording (relative to the cell's long axis), and n is the number of trajectories. During resuscitation experiments, the timing of resumption and possible cessation of PA movement was visually determined. Since expression of the *ibp* operon is strongly upregulated upon exposure to elevated temperatures, as it is part of the heat shock response of *E. coli* (Allen et al., 1992; Chuang and Blattner, 1993; Richmond et al., 1999), average cellular fluorescence increased and additional fluorescent foci occasionally appeared after heat treatment. This, however, did not impede monitoring of PA-movement. Please note that, regardless of the treatment, a small subfraction of cells (±3 %; (Govers and Aertsen, 2015)) did not contain any visible PAs, and as a consequence was not included in analyses examining/employing PA movement.

Determination of viability and resuscitation time measurements

Cellular viability (i.e. the relative number of resuscitated cells) was determined by time-lapse microscopy. Cells that could be observed to grow and divide within an 8 h time frame after heat treatment were scored as resuscitated cells. Please note that the detection limit for viability in these time-lapse microscopy samples varies between experiments and depends on the total number of observed cells, from 1/34 or 3.0 % to 1/127 or 0.8 %.

Cell meshes generated by the MicrobeTracker program were used to determine resuscitation times of individual cells, as described previously (Govers et al., 2014). Since bacterial cells typically only elongate in the longitudinal direction, resuscitation times were measured by looking at the length increase of individual cells over time. First, an initial length was calculated as the mean of the first three measurements for each individual cell. The length of that cell in the subsequent frames was then compared to this initial length, and the resuscitation time was defined as the time corresponding to the frame where cell length had increased over 10 % compared to its initial length, plus the time between the end of the heat treatment and the beginning of microscopy recording (typically around 15 min). Individual resuscitation times of cells exposed to a certain heat treatment were subsequently binned to create the cumulative resuscitation time distributions of MG1655 *ibpA-yfp* populations after a given heat treatment. The 10 % increase in initial length was taken as a threshold to prevent random measurement fluctuations from influencing the results and ensure that only resuscitation times of cells that had fully committed to growth were measured. In addition, only resuscitation times of cells that subsequently committed to growth and division were included.

Determination of persister fraction

To determine the persister fraction, cells (both control and heat-treated cells) were diluted (1/1000) into 50 ml of fresh LB medium containing ampicillin (100 µg/ml). At different time points, 1 ml samples were taken out, cells were harvested by centrifugation (4000 x g, 5 min) and resuspended in PBS. Subsequently, the persister fraction was determined through spot-plating experiments in which the appropriate dilutions of a sample were prepared in PBS and subsequently spot-plated (5 µl) on LB agar. After 24 h of incubation at 37°C, the plates were counted, and the number of survivors in CFU per ml (i.e. the persister fraction) was determined.

Acknowledgements

The authors would like to thank Ariel Lindner for providing the MGAY strain, Mark Rizzo for providing a plasmid encoding the mCerulean3 fluorescent protein, and Chris Michiels for providing helpful comments. This work was supported by a doctoral fellowship of the Flemish Agency for Innovation by Science and Technology (IWT-Vlaanderen to S.K.G.), by a postdoctoral fellowship of the Research Foundation of Flanders (FWO-Vlaanderen to E.G.), and by grants of the Research Foundation of Flanders (FWO-Vlaanderen; grant G.0580.11) and the KU Leuven Research Fund (IDO/10/012 and STRT1/10/036).

References

Ackermann, M. (2015) A functional perspective on phenotypic heterogeneity in microorganisms. *Nat Rev Microbiol* **13**: 497-508.

Allen, S.P., Polazzi, J.O., Gierse, J.K., and Easton, A.M. (1992) Two novel heat shock genes encoding proteins produced in response to heterologous protein expression in Escherichia coli. *J Bacteriol* **174**: 6938-6947.

Ayrapetyan, M., Williams, T.C., and Oliver, J.D. (2015) Bridging the gap between viable but non-culturable and antibiotic persistent bacteria. *Trends Microbiol* **23**: 7-13.

Balaban, N.Q., Merrin, J., Chait, R., Kowalik, L., and Leibler, S. (2004) Bacterial persistence as a phenotypic switch. *Science* **305**: 1622-1625.

Bertani, G. (2004) Lysogeny at mid-twentieth century: P1, P2, and other experimental systems. *J Bacteriol* **186**: 595-600.

Black, D.G., Ye, X.P., Harte, F., and Davidson, P.M. (2010) Thermal inactivation of Escherichia coli O157:H7 when grown statically or continuously in a chemostat. *J Food Prot* **73**: 2018-2024.

Booth, I.R. (2002) Stress and the single cell: intrapopulation diversity is a mechanism to ensure survival upon exposure to stress. *Int J Food Microbiol* **78**: 19-30.

Chuang, S.E., and Blattner, F.R. (1993) Characterization of twenty-six new heat shock genes of Escherichia coli. *J Bacteriol* **175**: 5242-5252.

Coquel, A.S., Jacob, J.P., Primet, M., Demarez, A., Dimiccoli, M., Julou, T. et al. (2013) Localization of protein aggregation in Escherichia coli is governed by diffusion and nucleoid macromolecular crowding effect. *PLoS Comput Biol* **9**: e1003038.

Davey, H.M. (2011) Life, death, and in-between: meanings and methods in microbiology. *Appl Environ Microbiol* **77**: 5571-5576.

Dobson, C.M. (2003) Protein folding and misfolding. *Nature* **426**: 884-890.

Fellows, P.J. (2000) *Food Processing Technology: Principles and Practice*. Cambridge: Woodhead Publishing Limited.

493 Fridman, O., Goldberg, A., Ronin, I., Shoresh, N., and Balaban, N.Q. (2014) Optimization of lag time
494 underlies antibiotic tolerance in evolved bacterial populations. *Nature* **513**: 418-421.
495 Gefen, O., and Balaban, N.Q. (2009) The importance of being persistent: heterogeneity of bacterial
496 populations under antibiotic stress. *FEMS Microbiol Rev* **33**: 704-717.
497 Gefen, O., Gabay, C., Mumcuoglu, M., Engel, G., and Balaban, N.Q. (2008) Single-cell protein induction
498 dynamics reveals a period of vulnerability to antibiotics in persister bacteria. *Proc Natl Acad Sci U S A* **105**:
499 6145-6149.
500 Ghosh, S., and Setlow, P. (2009) Isolation and characterization of superdormant spores of Bacillus species.
501 *J Bacteriol* **191**: 1787-1797.
502 Ghosh, S., Scotland, M., and Setlow, P. (2012) Levels of germination proteins in dormant and
503 superdormant spores of Bacillus subtilis. *J Bacteriol* **194**: 2221-2227.
504 Govers, S.K., and Aertsen, A. (2015) Impact of high hydrostatic pressure processing on individual cellular
505 resuscitation times and protein aggregates in Escherichia coli. *Int J Food Microbiol* **213**: 17-23.
506 Govers, S.K., Dutre, P., and Aertsen, A. (2014) In vivo disassembly and reassembly of protein aggregates
507 in Escherichia coli. *J Bacteriol* **196**: 2325-2332.
508 Ingham, C.J., Beerthuyzen, M., and van Hylckama Vlieg, J. (2008) Population heterogeneity of Lactobacillus
509 plantarum WCFS1 microcolonies in response to and recovery from acid stress. *Appl Environ Microbiol* **74**:
510 7750-7758.
511 Joers, A., Kaldalu, N., and Tenson, T. (2010) The frequency of persisters in Escherichia coli reflects the
512 kinetics of awakening from dormancy. *J Bacteriol* **192**: 3379-3384.
513 Joux, F., and Lebaron, P. (2000) Use of fluorescent probes to assess physiological functions of bacteria at
514 single-cell level. *Microbes Infect* **2**: 1523-1535.
515 Jozefczuk, S., Klie, S., Catchpole, G., Szymanski, J., Cuadros-Inostroza, A., Steinhauser, D. et al. (2010)
516 Metabolomic and transcriptomic stress response of Escherichia coli. *Mol Syst Biol* **6**: 364.

Kotte, O., Volkmer, B., Radzikowski, J.L., and Heinemann, M. (2014) Phenotypic bistability in Escherichia coli's central carbon metabolism. *Mol Syst Biol* **10**: 736.

Koutsoumanis, K.P., and Lianou, A. (2013) Stochasticity in colonial growth dynamics of individual bacterial cells. *Appl Environ Microbiol* **79**: 2294-2301.

Landgraf, D., Okumus, B., Chien, P., Baker, T.A., and Paulsson, J. (2012) Segregation of molecules at cell division reveals native protein localization. *Nat Methods* **9**: 480-482.

Lindner, A.B., Madden, R., Demarez, A., Stewart, E.J., and Taddei, F. (2008) Asymmetric segregation of protein aggregates is associated with cellular aging and rejuvenation. *Proc Natl Acad Sci U S A* **105**: 3076-3081.

Miller, J.H. (1992) *A short course in bacterial genetics : a laboratory manual and handbook for Escherichia coli and related bacteria*. Plainview, N.Y.: Cold Spring Harbor Laboratory Press.

Niven, G.W., Morton, J.S., Fuks, T., and Mackey, B.M. (2008) Influence of environmental stress on distributions of times to first division in Escherichia coli populations, as determined by digital-image analysis of individual cells. *Appl Environ Microbiol* **74**: 3757-3763.

Oliveira, S.M., Neeli-Venkata, R., Goncalves, N.S., Santinha, J.A., Martins, L., Tran, H. et al. (2015) Increased cytoplasm viscosity hampers aggregate polar segregation in Escherichia coli. *Mol Microbiol*.

Orman, M.A., and Brynildsen, M.P. (2015) Inhibition of stationary phase respiration impairs persister formation in E. coli. *Nat Commun* **6**: 7983.

Parry, B.R., Surovtsev, I.V., Cabeen, M.T., O'Hern, C.S., Dufresne, E.R., and Jacobs-Wagner, C. (2014) The bacterial cytoplasm has glass-like properties and is fluidized by metabolic activity. *Cell* **156**: 183-194.

Pasha, I., Saeed, F., Sultan, M.T., Khan, M.R., and Rohi, M. (2014) Recent developments in minimal processing: a tool to retain nutritional quality of food. *Crit Rev Food Sci Nutr* **54**: 340-351.

Richmond, C.S., Glasner, J.D., Mau, R., Jin, H., and Blattner, F.R. (1999) Genome-wide expression profiling in Escherichia coli K-12. *Nucleic Acids Res* **27**: 3821-3835.

Ryall, B., Eydallin, G., and Ferenci, T. (2012) Culture history and population heterogeneity as determinants of bacterial adaptation: the adaptomics of a single environmental transition. *Microbiol Mol Biol Rev* **76**: 597-625.

Sliusarenko, O., Heinritz, J., Emonet, T., and Jacobs-Wagner, C. (2011) High-throughput, subpixel precision analysis of bacterial morphogenesis and intracellular spatio-temporal dynamics. *Mol Microbiol* **80**: 612-627.

Soini, J., Falschlehner, C., Mayer, C., Bohm, D., Weinel, S., Panula, J. et al. (2005) Transient increase of ATP as a response to temperature up-shift in Escherichia coli. *Microb Cell Fact* **4**: 9.

Standaert, A.R., Francois, K., Devlieghere, F., Debevere, J., Van Impe, J.F., and Geeraerd, A.H. (2007) Modeling individual cell lag time distributions for Listeria monocytogenes. *Risk Anal* **27**: 241-254.

Strauber, H., and Muller, S. (2010) Viability states of bacteria--specific mechanisms of selected probes. *Cytometry A* **77**: 623-634.

Stringer, S.C., Webb, M.D., George, S.M., Pin, C., and Peck, M.W. (2005) Heterogeneity of times required for germination and outgrowth from single spores of nonproteolytic Clostridium botulinum. *Appl Environ Microbiol* **71**: 4998-5003.

Veening, J.W., Stewart, E.J., Berngruber, T.W., Taddei, F., Kuipers, O.P., and Hamoen, L.W. (2008) Bet-hedging and epigenetic inheritance in bacterial cell development. *Proc Natl Acad Sci U S A* **105**: 4393-4398.

Weber, S.C., Spakowitz, A.J., and Theriot, J.A. (2012) Nonthermal ATP-dependent fluctuations contribute to the in vivo motion of chromosomal loci. *Proc Natl Acad Sci U S A* **109**: 7338-7343.

Wesche, A.M., Gurtler, J.B., Marks, B.P., and Ryser, E.T. (2009) Stress, sublethal injury, resuscitation, and virulence of bacterial foodborne pathogens. *J Food Prot* **72**: 1121-1138.

Winkler, J., Seybert, A., Konig, L., Pruggnaller, S., Haselmann, U., Sourjik, V. et al. (2010) Quantitative and spatio-temporal features of protein aggregation in Escherichia coli and consequences on protein quality control and cellular ageing. *EMBO J* **29**: 910-923.

Ye, Y., Zhang, L., Hao, F., Zhang, J., Wang, Y., and Tang, H. (2012) Global metabolomic responses of Escherichia coli to heat stress. *J Proteome Res* **11**: 2559-2566.

Figure legends

Figure 1. The mobility of intracellular PAs is affected by metabolic activity.

(A-C) Representative images of a time-lapse fluorescence microscopy image sequence of *E. coli* MG1655 *ibpA-yfp* cells on (A) LB medium, (B) LB medium with 20 µM CCCP, and (C) PBS buffer with 20 µM CCCP. The corresponding phase contrast images are superimposed with YFP epifluorescence images visualizing intracellular PAs. The scale bar corresponds to 1 µm. (D-F) Two-dimensional trajectories representing 3 min of IbpA-YFP tracking from the single *E. coli* cells depicted in (A-C). (G) MSD of IbpA-YFP structures in control cells on LB medium (n = 380), cells exposed to 20 µM CCCP on LB medium (n = 267), and cells exposed to 20 µM CCCP on PBS (n = 480).

Figure 2. Bacterial inactivation, resuscitation time and heterogeneity increase with the severity of the heat treatment.

(A) Cumulative resuscitation time distributions of MG1655 *ibpA-yfp* cells after indicated heat treatments (15 min). The time individual resuscitating cells needed to resume growth, defined as the ability of cells to resume growth and subsequent division within 8 hours after a certain heat treatment, was determined and binned to create the cumulative lag time distributions. For each temperature, the mean cumulative lag time distribution of three independent experiments is shown. Please note that the cumulative lag time distributions take the fraction of resuscitating cells into account and that, per applied temperature, the

589 total number of observed cells per independent experiment varies (n ≥ 37 for control cells, n ≥ 112 for
590 cells exposed to 51 °C, n ≥ 199 for cells exposed to 52 °C, n ≥ 149 for cells exposed to 53 °C, n ≥ 284 for
591 cells exposed to 54 °C and n ≥ 211 for cells exposed to 55°C). (B) Correlation between the average cellular
592 resuscitation time for cells after a certain heat treatment and their standard deviation. The positive
593 correlation (Pearson's r = 0.9922, p-value = 8.94×10^{-5}) implies a more heterogeneous growth resumption
594 pattern with increasing average cellular resuscitation time, and thus, with increasing temperature. (C)
595 Representative TLFM images of resuscitating *E. coli* MG1655 *ibpA-yfp* cells after heat treatment (53°C, 15
596 min) illustrating the observed heterogeneity in resuscitation times and PA movement. The black arrow
597 indicates a cell that initiates PA movement, but is unable to resume growth nor subsequent division. The
598 corresponding phase contrast images are superimposed with YFP epifluorescence images visualizing
599 intracellular PAs. The scale bar corresponds to 2 µm.

600

601 **Figure 3**. PA movement in resuscitating and non-resuscitating cellular subfractions.

602

603 Fraction of *E. coli* MG1655 *ibpA-yfp* cells displaying PA movement after the indicated heat treatment (15
604 min). The relative contribution of resuscitating (dark grey bars), here defined as the ability of cells to
605 resume growth and subsequent division within 8 hours after heat treatment, and non-resuscitating (light
606 grey bars) cells to the total number of cells displaying PA movement (black bars) is shown. The means of
607 three independent experiments are shown with error bars representing the standard deviation. Please
608 note that, per temperature, the total number of observed cells per independent experiment, and thus
609 also the detection limit varies (see Fig. 2A).

610

611 **Figure 4**. Intracellular PA movement highlights individual cellular fates in heat stressed (53 °C, 15 min)
612 populations.

(A) Behavior of individual cells of *E. coli* MG1655 *ibpA-yfp* monitored with TLFM for 8 h after heat treatment, with indication of the absence (dark colors) or presence (light colors) of PA movement, and the eventual fate (red = non-resuscitated, blue = resuscitated). The data stem from three independent experiments with n ≥ 149 per independent experiment. Each horizontal line represents the behavior of a single cell. The overall fraction of cells belonging to a certain group or subgroup is indicated between parentheses. (B) Distribution of PA movement initiation time in metabolically active but non-resuscitating cells of panel A. The time at which non-resuscitating cells initiated PA movement was determined and binned to create the distribution. (C) Same as (B) but for resuscitating cells. (D) Resuscitation time distribution of resuscitating cells of panel A. The time individual cells needed to resume growth after heat treatment was determined and binned to create the resuscitation time distribution. (E) Correlation between the time resuscitating cells of panel A need to initiate PA movement and their respective resuscitation time (Pearson's r = 0.3479, p-value = 1.94×10^{-5}). The bisector is shown as a dashed line. (F-L) Representative TLFM images of particular cells of panel A showing different fates at the indicated times after heat stress. The corresponding phase contrast images are superimposed with YFP epifluorescence images visualizing intracellular PAs. The group to which a cell belongs at a given time point is indicated in the top right corner of each image. The scale bar corresponds to 1 µm.

Figure 5. Metabolically active but non- resuscitating cells can initiate gene expression and protein translation.

Behavior of *E. coli* MG1655 *ibpA-yfp* cells equipped with a pTrc99A-P_{trc}-*mCer3* expression construct after heat treatment (53 °C, 15 min) on LB agarose pads containing 1 mM IPTG. Representative images of a

TLFM image sequence of a (A) resuscitating and (B) non-resuscitating but metabolically active cell performing gene expression and translation at the indicated time after heat stress are shown. The corresponding phase contrast images are superimposed with YFP epifluorescence images visualizing intracellular PAs. Below, CFP epifluorescence images of that same time-lapse fluorescence microscopy image sequence, displaying inducible gene expression (upon the addition of 1 mM IPTG), are shown. The scale bar corresponds to 1 µM. (C) Graphs displaying the evolution of relative cell length (grey lines) and relative total cellular fluorescence (blue lines) of all observed non-resuscitating but metabolically active cells. Each black rectangle represents a single cell.

Figure 6. Metabolically active but non-resuscitated cells are able to persist in the presence of ampicillin (100 µg/ml).

Representative TLFM images at indicated time points of (A) unstressed control cells of *E. coli* MG1655 *ibpA-yfp* rapidly lysed by the ampicillin incorporated in the LB agarose pad embedding the cells, in contrast to (B) heat stressed (53 °C, 15 min) cells where resuscitation postpones lysis by ampicillin. Please note that different time points are shown in (A) and (B). (C-F) Representative TLFM images at indicated time points of metabolically active but (seemingly) non-resuscitating heat stressed *E. coli* MG1655 *ibpA-yfp* cells either (C, D) ceasing PA movement or (E, F) losing structural integrity in the continued presence of ampicillin. Both categories contained individuals able to sustain PA movement for more than 24 hours (D, F). The corresponding phase contrast images are superimposed with YFP epifluorescence images visualizing intracellular PAs. The scale bar corresponds to 1 µm. (G) Curve indicating the fraction of metabolically active but (seemingly) non-resuscitating heat stressed *E. coli* MG1655 *ibpA-yfp* cells retaining PA movement upon prolonged TLFM monitoring in the continued presence of ampicillin (100 %

represents 28 cells observed with TLFM for 8 h after heat exposure). (H) Survival kinetics of control and heat-treated (53 °C, 15 min) *E. coli* MG1655 *ibpA-yfp* cells inoculated (1/1000) into fresh LB medium containing 100 µg/ml ampicillin. Dotted line indicates the detection limit of 2 x 10^2 CFU/ml. (I) Images of an LB agar plate containing an appropriate dilution of heat stressed (53 °C, 15 min) *E. coli* MG1655 *ibpA-yfp* cells after 72 h of incubation. Arrows indicate two late-appearing colonies (out of a total of 144) that were not visible after 24 h of incubation.

Figures

Figure 1

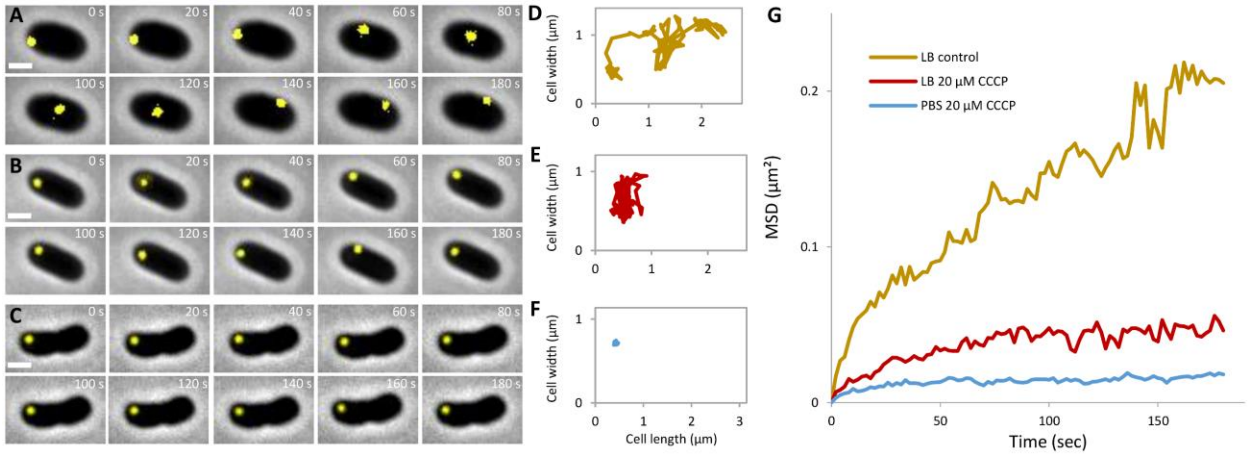

671 Figure 2

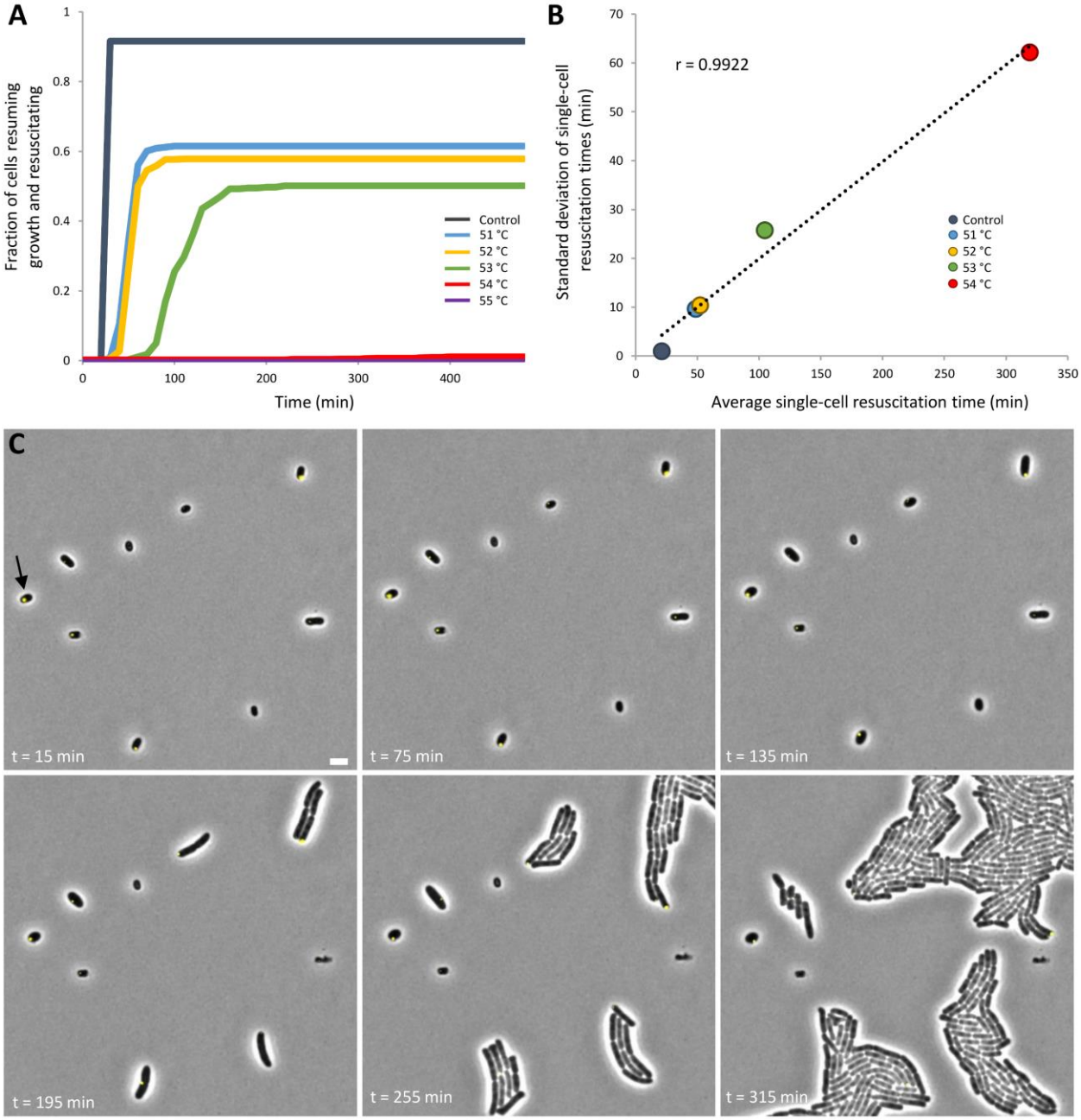

672

673 Figure 3

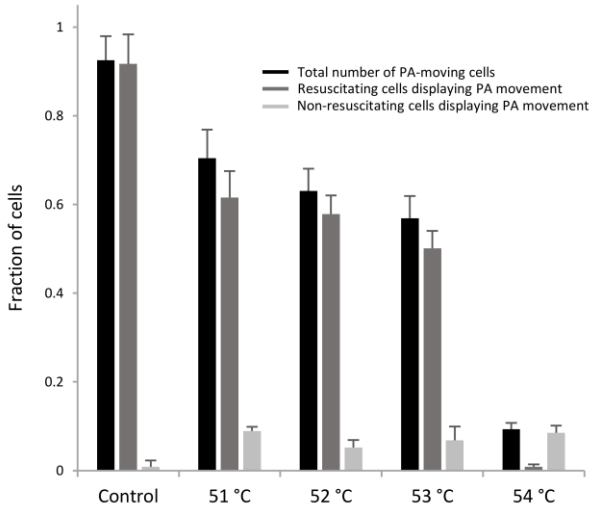

674

675 Figure 4

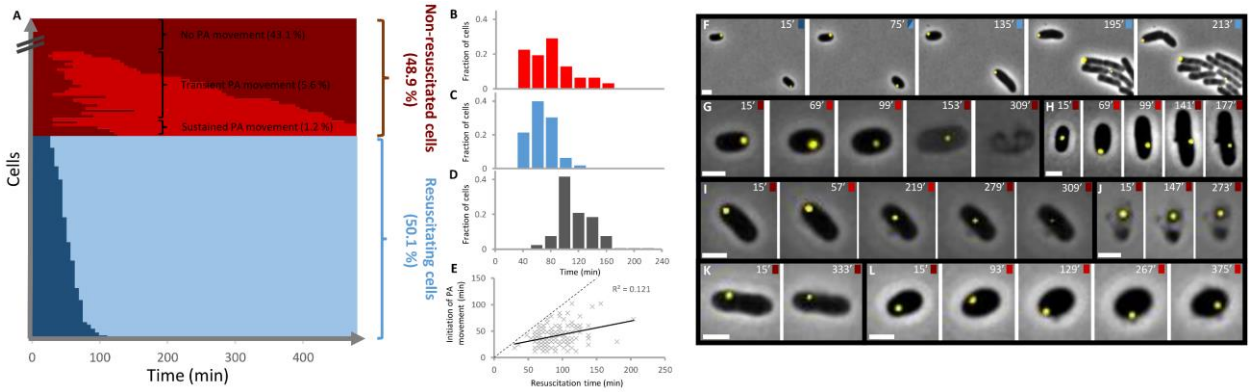

676

677 Figure 5

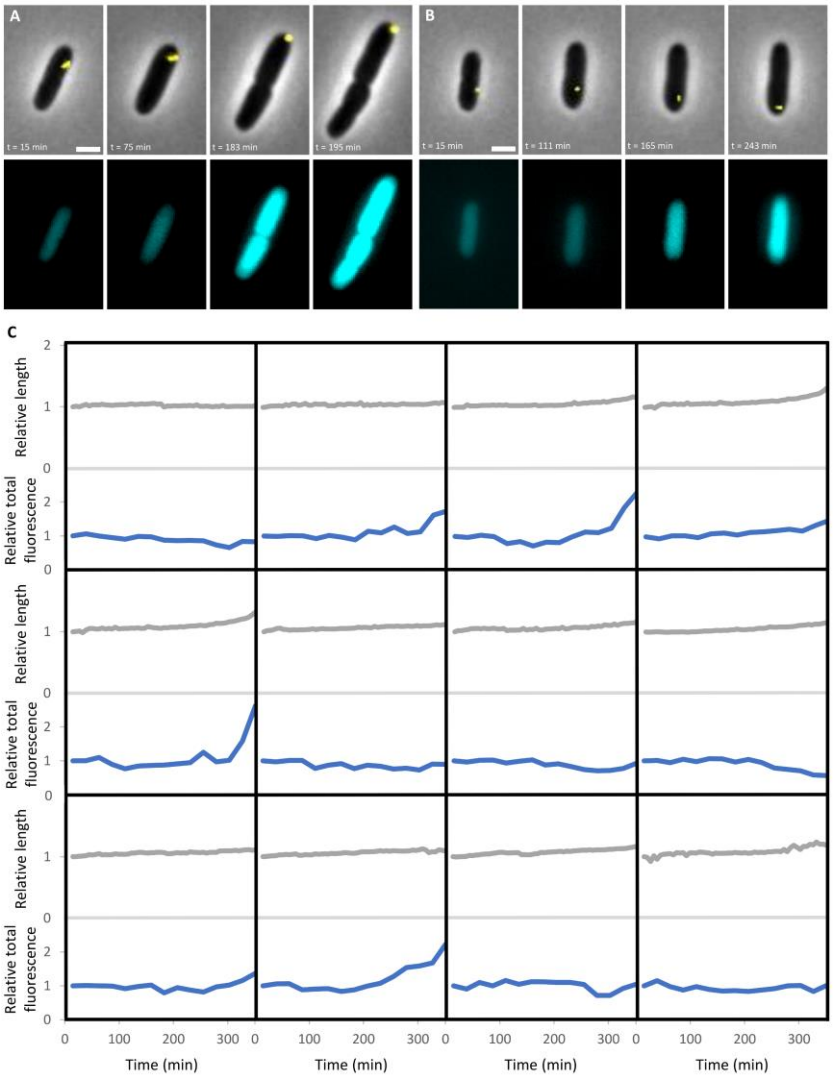

678

679 Figure 6

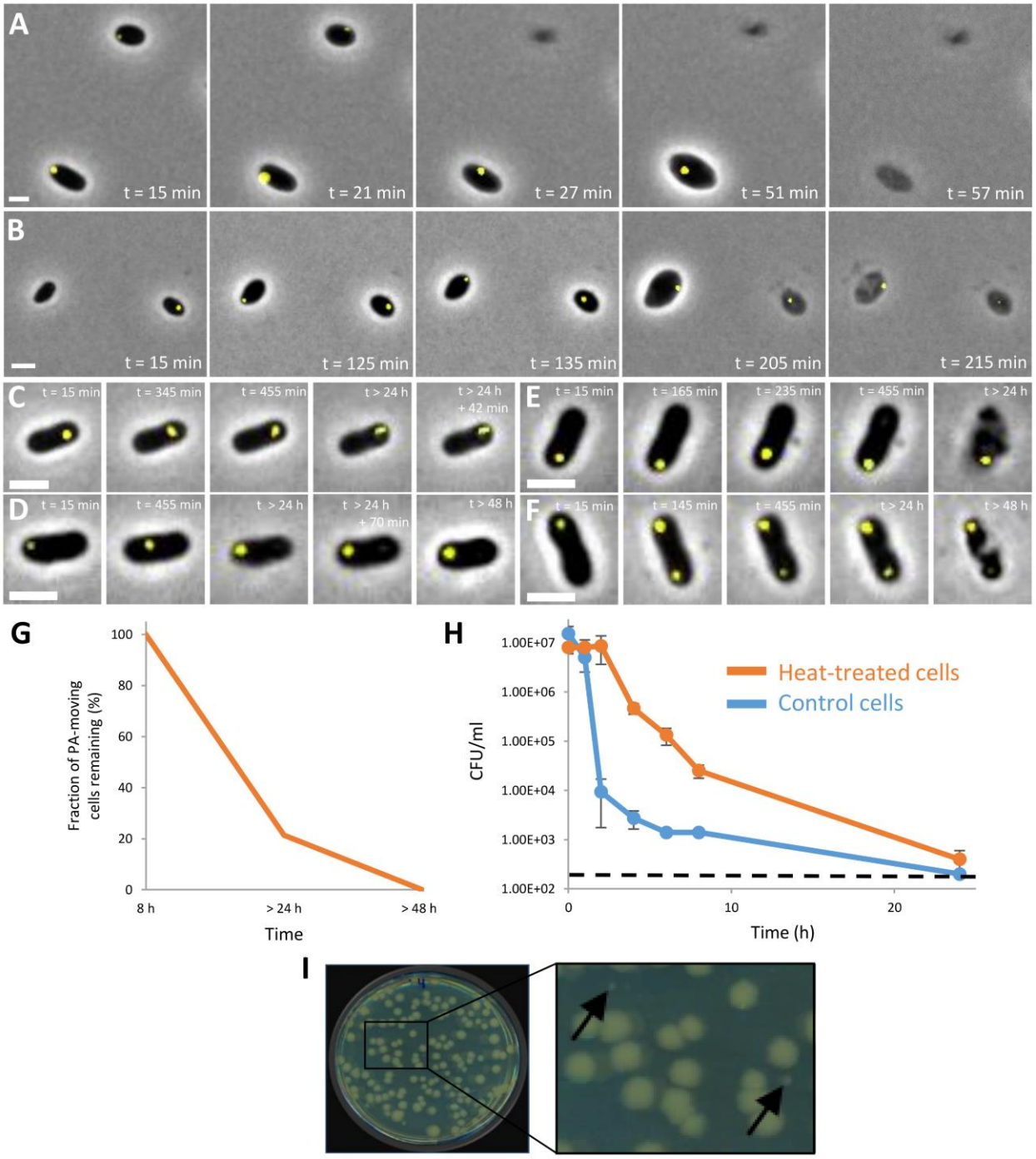

680

681

682

683

684

Supporting information

Figure S1. The mobility of intracellular PAs is also affected by metabolic activity in exponentially growing *E. coli* cells.

MSD of IbpA-YFP structures in exponential phase on LB medium (n = 179), cells exposed to 20 µM CCCP on LB medium (n = 194), and cells exposed to 20 µM CCCP on PBS (n = 49).

Figure S2. Intracellular PA movement highlights individual cellular fates in HHP stressed (300 MPa, 15 min, 20 °C) populations.

(A) Behavior of individual cells of MG1655 *ibpA-yfp* monitored with TLFM for 8 h after HHP treatment, with indication of the absence (dark colors) or presence (light colors) of PA movement, and the eventual fate (red = non-resuscitated, blue = resuscitated). The data stem from three independent experiments with n ≥ 1011 per independent experiment. A small fraction of resuscitating cells (1.5 % of total cells) already displayed PA movement at the beginning of recording, approximately 15 min after HHP treatment (alternating dark and light blue). Each horizontal line represents the behavior of a single cell. The overall fraction of cells belonging to a certain group or subgroup is indicated between parentheses.

(B) Representative TLFM images of particular cells of panel A showing different fates at the indicated time after HHP stress. The corresponding phase contrast images are superimposed with YFP epifluorescence images visualizing intracellular PAs. The group to which a cell belongs at a given time point is indicated in the top left corner of each image. YFP epifluorescence images (reporting PAs) in combination with cell outlines are shown at the indicated times after HP exposure. The scale bar corresponds to 1 µm (please note that every row is shown on a different scale, and that the two last images of the last row are also shown on a different scale).

Supplemental figure 1

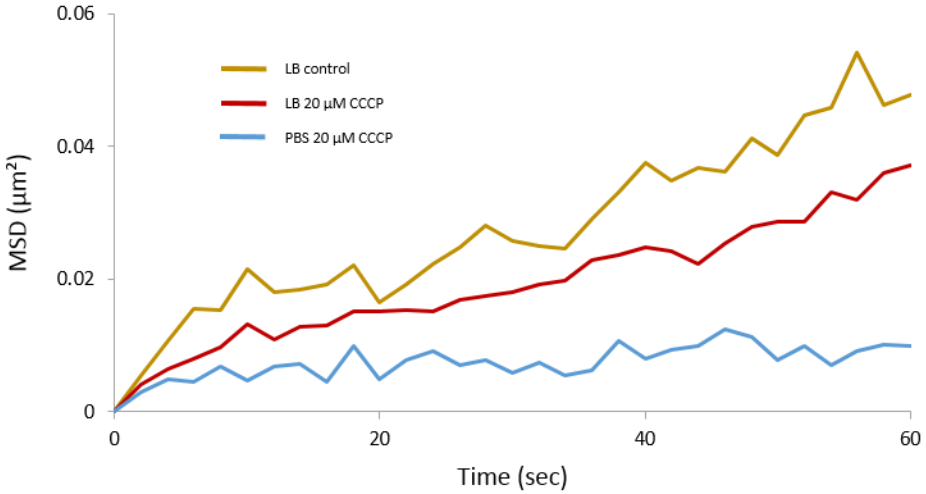

741
742
743
744
745

Supplemental figure 2